Journal of South American Earth Sciences 51 (2014) 1–11

Contents lists available at ScienceDirect

Journal of South American Earth Sciences

journal homepage: www.elsevier.com/locate/jsames

# Seismicity distribution in the vicinity of the Chile Triple Junction, Aysén Region, southern Chile

Hans Agurto-Detzel [a,*], Andreas Rietbrock [a], Klaus Bataille [b], Matthew Miller [c], Hikaru Iwamori [d], Keith Priestley [e]

[a] Department of Earth, Ocean and Ecological Sciences, University of Liverpool, Jane Herdman Building, Liverpool L69 3GP, United Kingdom
[b] Department of Earth Sciences, University of Concepción, Chile
[c] Department of Geophysics, University of Concepción, Chile
[d] Department of Earth and Planetary Sciences, Tokyo Institute of Technology, Japan
[e] Bullard Laboratories, University of Cambridge, UK

ARTICLE INFO

*Article history:*
Received 6 May 2013
Accepted 23 December 2013

*Keywords:*
Chile
Aysen
Local seismicity
Liquiñe-Ofqui fault
Chile Triple Junction
Hudson volcano

ABSTRACT

The Aysén Region, southern Chile, is the area located at the southern end of the Nazca-South America subduction zone, to the east of the Chile Triple Junction. This region has historically presented low levels of seismicity mostly related to volcanism. Nonetheless, a seismic sequence occurred in 2007, related to the reactivation of the strike-slip Liquiñe-Ofqui Fault System (LOFS), confirmed that this region is not exempt from major seismic activity M ~ 7. Here we present results from background local seismicity of two years (2004–2005) preceding the sequence of 2007. Event magnitudes range between 0.5 and 3.4 $M_L$ and hypocenters occur at shallow depths, mostly within the upper 10 km of crust, in the overriding South American plate. No events were detected in the area locus of the 2007 sequence, and the Wadati–Benioff (WB) plane is not observable given the lack of subduction inter-plate seismicity in the area. A third of the seismicity is related to Hudson volcano activity, and sparse crustal events can be spatially associated with the trace of the Liquiñe-Ofqui fault, showing the largest detected magnitudes, in particular at the place where the two main branches of the LOFS meet. Other minor sources of seismicity correspond to glacial calving in the terminal zones of glaciers and mining explosions.



## 1. Introduction

The Aysén Region, southern Chile, is located within the southern end of the rupture area of the Great 1960 Valdivia earthquake (Plafker and Savage, 1970), making of this region an area prone to tsunami hazard. Nevertheless, the Aysén region lacks of major teleseismic recordings and in general only presents sparse seismicity of intra-plate crustal origin.

This region correspond to an interesting seismotectonic environment as it is bisected by a large strike-slip fault system, the Liquiñe-Ofqui fault system (LOFS), which absorbs the trench-parallel component of the oblique convergence between Nazca and South American plates. In addition, the current subduction of an active spreading center, the Chile Ridge, has generated the presence of an asthenospheric slab window beneath the overriding continental plate (Russo et al., 2010a).

Recently in 2007, the area was locus of an earthquakes sequence related to the reactivation of the LOFS, with a peak of activity given by a $M_W$ 6.2 earthquake that generated a landslide-induced local tsunami killing 10 people. The area affected in 2007 is of particular economic interest given the presence of salmon farms and hydro-electric resources.

Little is known about the local seismicity in this region. One important problem is the lack of local seismic studies covering the whole of the region, and the absence of maximum possible magnitudes at any given sector. Furthermore, the sources for local seismicity have not been clearly established. The geometry of the Wadatti–Benioff plane is well constrained from 43°S northwards, but not for the region south of it where the actual southern end of the Western-South America subduction margin is located.

The goal of the present study is to determine the seismicity pattern of the Aysén region and establish its main sources of activity previous to the sequence of 2007. Specific questions (objectives) we want to address are:

* Corresponding author. Present address. Institute of Astronomy, Geophysics and Atmospheric Sciences, University of São Paulo, Rua do Matão, 1226 – Cid. Universitária São Paulo, 05508-090 SP, Brazil. Tel.: +55 11 30912789.
*E-mail addresses:* h.agurto.detzel@gmail.com, hans@iag.usp.br (H. Agurto-Detzel), a.rietbrock@liverpool.ac.uk (A. Rietbrock), bataille@udec.cl (K. Bataille), m.miller@dgeo.udec.cl (M. Miller), hikaru@geo.titech.ac.jp (H. Iwamori), kfp10@cam.ac.uk (K. Priestley).

0895-9811/$ – see front matter © 2014 Elsevier Ltd. All rights reserved.
http://dx.doi.org/10.1016/j.jsames.2013.12.011

1. What is the spatial distribution of earthquakes in the region and their magnitudes?
2. What are the sources of seismicity in the region?
3. Is there WB seismicity occurring? If not, why?
4. What are the effects of the main present tectonic features (e.g. slip partitioning and subduction of young lithosphere and an active ridge) on the upper plate deformation and associated seismicity pattern?
5. What are the possible maximum magnitudes at given areas of the region.
6. Was there any previous indication of seismicity in the area affected by the 2007 Aysén Fjord sequence?

Kirby et al. (1996) proposed that subduction of very young lithosphere (<15–25 Ma) and high heath flow (as in the case of the Aysén Region) produces mainly shallow earthquakes and sparse or absent volcanism. We hypothesize that seismicity in the Aysén Region occurs only at shallow depths (<~30 km), presenting low magnitudes and an absent or poorly defined WB zone. Occasionally though, maximum magnitudes in the region could reach M ~ 7 as demonstrated by the recent Aysén Fjord events related to the LOFS and an earthquake occurred in 1927 (see below).

In order to tackle these issues, data from an extensive local network deployed during 2004–2005 (Miller et al., 2005) is analyzed. We benefit from the usage of a recently derived 1-D local velocity model for the area (Agurto et al., 2012) and a non-linear location method (NonLinLoc, Lomax et al., 2000) to obtain accurate earthquake locations and associated uncertainties.

### 1.1. Location and geo-tectonic setting

The study region is located at the southern end of the subductive convergent margin between the Nazca and South American plates (Fig. 1), where the active Chile Ridge is currently subducting offshore of the Taitao Peninsula (Herron et al., 1981; Cande et al., 1987) at the so-called Chile Triple Junction (CTJ). This tectonic configuration corresponds to the only present-day active ridge-trench collision in which the overriding plate represents continental lithosphere. North of the CTJ, a young and buoyant portion of the Nazca plate is being subducted at a rate of 6.6 cm $yr^{-1}$, while to the south, the Antarctic plate is being subducted at 2 cm $yr^{-1}$ below South America (Wang et al., 2007).

Several consequences of the Chile Ridge subduction beneath the CTJ have been observed including: tectonic erosion, plutonism near the trench and uplift during the Upper Cretaceous in the Taitao Peninsula (Cande and Leslie, 1986), emplacement of an ophiolitic complex in the Taitao Peninsula (Forsythe et al., 1986) and the displacement of a fore-arc sliver (Forsythe and Nelson, 1985; Wang et al., 2007). Another important consequence is the occurrence of a 350 km long volcanic gap within the arc (Ramos and Kay, 1992), whilst in the back-arc zone widespread basaltic-plateau volcanism takes place (e.g. Ramos and Kay, 1992; Gorring et al., 1997). Ramos and Kay (1992) argue that the most intense periods of this basaltic volcanism are related to the passage of a slab window (subducted ridge) below the plateau.

The WB seismicity observed along the southern Chile convergent margin decreases in terms of quantity and depth of subduction events from north to south until the CTJ where the age of the

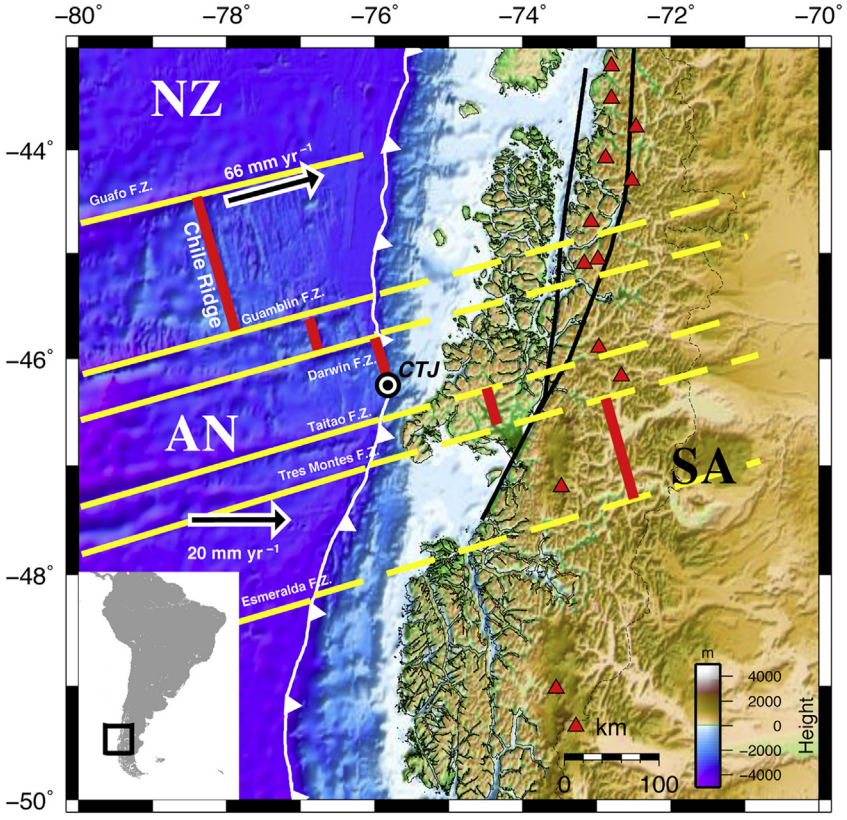


**Fig. 1.** Location and tectonic settings of the Aysén Region. NZ Nazca plate; AN Antarctic plate; SA South American plate; CTJ Chile Triple Junction. White line with triangles indicate the trench. Red segments show spreading centers of the Chile Ridge and their projection after subducted. Yellow lines indicate fracture zones (solid yellow lines) and their projection (dashed yellow lines). Black line depicts the Liquiñe-Ofqui Faults System (LOFS), while red triangles indicate Quaternary volcanoes. Bathymetry/Topography: GTOPO30; convergence NZ and AN: Wang et al. (2007). (For interpretation of the references to color in this figure legend, the reader is referred to the web version of this article.)

subducting slab is nearly ~0 Ma. Several authors have established a direct relationship between the distribution of WB seismicity and the age of the subducting slab (e.g. Wortel and Vlaar, 1978; Kirby et al., 1996), indicating that the subduction of a very young oceanic crust would prevent the occurrence of deep subduction seismicity. The lack of teleseismic events south of 43°S has made difficult to clearly define the geometry of the WB zone south of this latitude. Northwards, Bohm et al. (2002) defined a clear WB zone dipping 30° to the east, with earthquakes down to 150 km depth for the segment between 36 and 40°S. Using a local seismic arrangement, Lange et al. (2007) found subduction seismicity between 12 and 70 km depth for the segment contained between 41.5° and 43.5°S, with a WB zone dipping 30°–33° to the east.

The Aysén region is crossed by a major crustal structure, the LOFS, which corresponds to a dextral strike-slip NNE-striking fault system that extends for more than 1000 km along the arc. It is formed by two main NNE-trending parallel lineaments connected by at least four NE-trending en échelon lineaments that define a strike-slip duplex (Cembrano et al., 1996, Fig. 2). This fault system accommodates part of the strike-parallel component of oblique convergence between the Nazca and the South American plate and it is thought to control the distribution of Quaternary volcanism in the area (Cembrano and Moreno, 1994; Cembrano and Lara, 2009).

Most of the information on the current deformation state of the LOFS comes from structural and thermo-chronological evidence (e.g. Cembrano et al., 1996, 2000, 2002; Thomson, 2002) which suggest that this fault has been active since Late Mesozoic as a sinistral strike-slip fault, while the dextral strike-slip motion is dated to begin about Middle Miocene. Strike-slip brittle deformation during the Pliocene to post-Pliocene and high rates of uplift during the Holocene characterize the recent tectonics of the LOFS (Cembrano et al., 1996). Based on structural field work and fault kinematic analysis, Rosenau et al. (2006) determined intra-arc shear rates from the Pliocene to recent period of 32 ± 6 mm $yr^{-1}$ for the southern portion of the LOFS between 40° and 42°S and of 13 ± 3 mm $yr^{-1}$ for the northern portion between 38° and 40°S. These rates implicate that about half of the plates' convergence obliquity is accommodated in the arc by the LOFS in the northern segment of their study (38°–40°S), while complete partitioning occurs in the southern portion (40°–42°S). Furthermore, these authors suggest that where partitioning is incomplete, the convergence obliquity is accommodated by oblique interplate thrusting and forearc transpression.

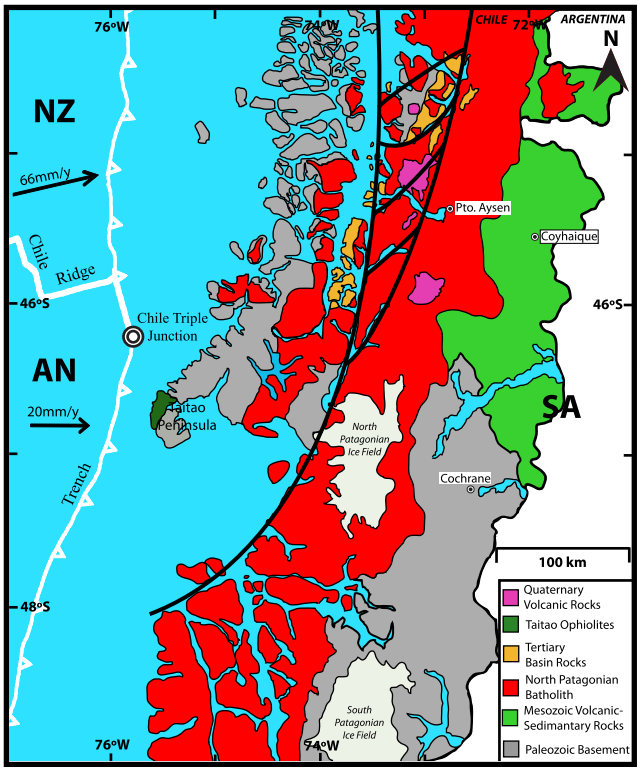


**Fig. 2.** Simplified geology of the Aysén Region. Black line shows the trace of the LOFS. Other features see Fig. 1. Modified from SERNAGEOMIN (2003).

Wang et al. (2007) reported the first geodetic evidence on the current dextral shear of the LOFS, finding a trench-parallel slip rate of 6.5 mm $yr^{-1}$ between 42° and 44°S, which accommodates about 75% of the current margin-parallel component of the Nazca-South America relative plate motion. Lange et al. (2008) observed local crustal seismicity along a 130 km long segment of the fault at ~42°S. At this latitude, the Chiloé block mentioned above has been decoupled from South America by the action of the LOFS (Forsythe and Nelson, 1985; Wang et al., 2007; Melnick et al., 2009).

The geology of the Aysén Region is most simply defined by three predominantly N–S trending domains: a western coastal domain, a central plutonic belt and an eastern back-arc volcano-sedimentary domain (Fig. 2). The morpho-structural setting is controlled by NE–SW and NW–SE structures related to the LOFS (D'Orazio et al., 2003). The coastal domain is mainly characterized by Palaeozoic and Triassic metamorphic rocks located on the archipelago islands. Additionally, an ophiolite complex was emplaced within the fore-arc about 3 Ma in the Taitao Peninsula (Forsythe et al., 1986). This ophiolite accretion and anomalous near-trench magmatism are most likely related to the passage of the CTJ at the latitude of the Taitao Peninsula ~3 Ma (Behrmann et al., 1994). A granitic plutonic belt of Meso-Cenozoic age, the North Patagonian Batholith, is located between 40° and 47° lat. S, encompassing the Main Cordillera of the Andes and the eastern portion of the Coastal Cordillera (Pankhurst et al., 1999), and including the highest altitudes in the area (up to 2000 m.a.s.l.). Quaternary volcanism is also present in the region with strato-volcanoes Hudson, Maca, Cay and several monogenetic cones, which occur over the volcanic arc (D'Orazio et al., 2003). The active Hudson volcano had its last major eruption on August 1991, producing more than 4 $km^3$ of pyroclastic material transported in NE direction (Naranjo and Stern, 1998). To the east, the back-arc zone is composed mainly of Meso-Cenozoic volcano-sedimentary rocks and the eastern outcrop of the Paleozoic basement (Niemeyer et al., 1984; SERNAGEOMIN, 2003).

### 1.2. Previous seismic studies in the region

Considering the available information, the Aysén Region has a poor catalogue of seismic events partially due to the lack of local studies, difficulties of conducting field work, and/or the low rates of seismicity. According to the Chilean Seismological Survey (http://sismologia.cl), only one historical event $M > 7$ has been observed in the time period from 1570 to 2005. This event, magnitude 7.1, occurred on November 21, 1927, (Greve, 1964) to the West of the Aysén Fjord causing a local tsunami. The teleseismically-recorded major seismicity of the area (e.g. Global Centroid Moment Tensor catalog and NEIC-PDE catalog) is directly linked to the present main tectonic processes: (1) the subduction of the Nazca plate under South America to the north of the CTJ and (2) the ocean floor spreading along the Chile Ridge. Additionally, intraplate seismicity in the overriding plate can be associated with deformation on the LOFS (e.g. Lange et al., 2008; Agurto et al., 2012) and active volcanism in the arc, in particular the Hudson volcano.

Only a few local seismic networks have been installed in the Aysén Region. Murdie et al. (1993) deployed nine seismometers in

the Taitao Peninsula between February and March 1992, locating around 50 events with magnitudes from 0 to 4 close to the CTJ. Miller et al. (2005) maintained the first local seismic network throughout the whole Aysén Region between January 2004 to February 2006 detecting only minor crustal seismicity.

Comte et al. (2007) deployed a temporal seismic network in the region allowing them to capture the initial phases of the Aysén seismic sequence of 2007. Using the same local network, Russo et al. (2010a) produced body-wave travel-time tomography, imaging and confirming the existence of an asthenospheric slab window beneath the overriding plate, produced by the subduction of the Chile active spreading center. Gallego et al. (2010) produced seismic noise tomography for the region, obtaining high crustal shear-wave velocities in outcrop areas of the North Patagonian Batholith and highly compacted metamorphic rocks, while low shear-wave velocities were found along the volcanic arc and trace of the LOFS.

Using teleseismic arrivals of S-waves radiated from six of the largest events of the 2007 Aysén seismic sequence, Russo et al. (2010b) studied shear wave splitting and upper mantle flow of this region. Their results show a transition from the generally N–S-trending fast shear wave azimuths north of the CTJ, to ENE-trending azimuths in the area of the asthenospheric slab window mentioned before. They interpreted this ENE-trend as the flow of Pacific Basin upper mantle from the west, eastward beneath South America. This flow then interacts with the mantle wedge present above the asthenospheric window to produce the extensive basaltic plateau located at the east of Chile and in Argentina in this region.

Finally, several authors investigated the 2007 Aysén seismic sequence (e.g. Sepúlveda and Serey, 2009; Mora et al., 2010; Legrand et al., 2011; Russo et al., 2011; Agurto et al., 2012). These last authors deployed a small seismic network around the Aysén Fjord, inferring a tectonic origin for the sequence and deriving a new local velocity model for the area.

## 2. Data and methods

During 2004 and 2005 a local seismic network (Miller et al., 2005) of more than 60 broadband and short-period stations was kept continuously recording in the Aysén Region (Figs. 3 and 4). Data from this network was obtained and analyzed for the present work, addressing the local seismicity pattern in the region. Due to the extremely difficult accessibility and weather conditions for many of the deployment sites, the network's recording was not homogeneous, with dead stations present mostly during the winter months. The performance of the network therefore was not the best, and although the high number of total stations involved in the project, many events were only recorded by less than 10 stations. Moreover, as the main objective of the network installation was to investigate the crustal and upper mantle structure of the region, the network configuration was not ideal to constrain the local seismicity distribution of the whole region. Fig. 3 shows number of events detected and active stations per day during the deployment period. Whilst the first year only 8 to 14 stations were active, the number of detected events per day is similar to that of the second year of deployment, when up to four times more stations were active. This indicates that even with the smaller deployment of the first year, the network was capable of detecting the weak seismicity of the region without missing small events ($\sim$2.5 $M_L$).

The continuous data was visually scanned, and then P- and S-wave arrival times were manually determined for a total of 519 events. In order to obtain event locations, arrival times were processed with the software NonLinLoc (Lomax et al., 2000), which provides non-linear probabilistic locations with a complete determination of the posterior probabilistic density function (pdf), thus computing reliable location uncertainties. A recently published 1-D velocity model for the area (Agurto et al., 2012; see Table 1) was used for this instance.

## 3. Local seismicity

Considering all detected events, i.e. 519, an average of 1.35 seismic events per day occur in the Aysén Region. The temporal distribution (Fig. 3) shows for most of the days the occurrence of 1–2 events, with a slightly greater concentration of events during the first months of study (January–May 2004).

Only events with uncertainty ellipsoid semi-axes smaller than 20 km were considered for the following analysis, reducing the number of events from 519 to 276. In average 15 observations per event (P and S phases) were picked for this selection. Uncertainty estimations are shown in Figs. 4 and 5. As expected, the smallest location errors ($<\pm$4 km) are found for those events located within the network, while larger errors ($>\pm$10 km) are present for events outside and away from the seismic network. The orientation of 68% confidence ellipsoids do not show any

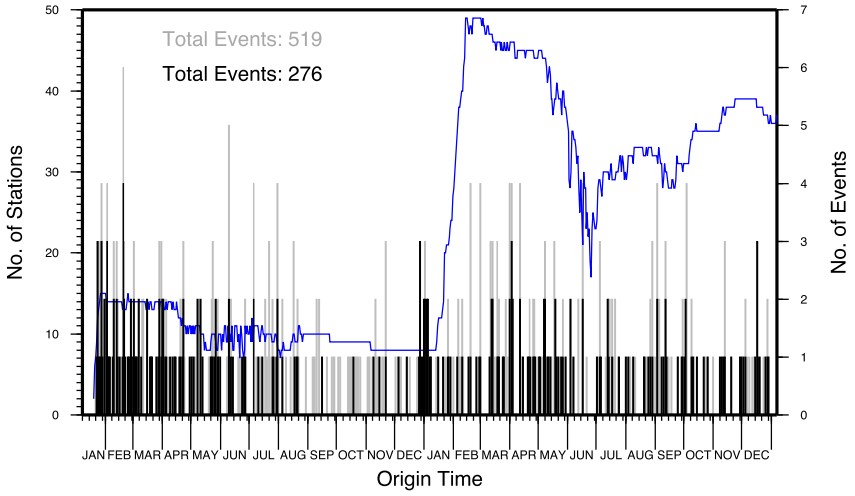


**Fig. 3.** Events occurrence and active stations per day. Events associated with mining activities have been filtered out. Gray bars show total events processed, black bars show events in Fig. 4 (right axis). Blue thin line shows number of active stations (left axis). (For interpretation of the references to color in this figure legend, the reader is referred to the web version of this article.)

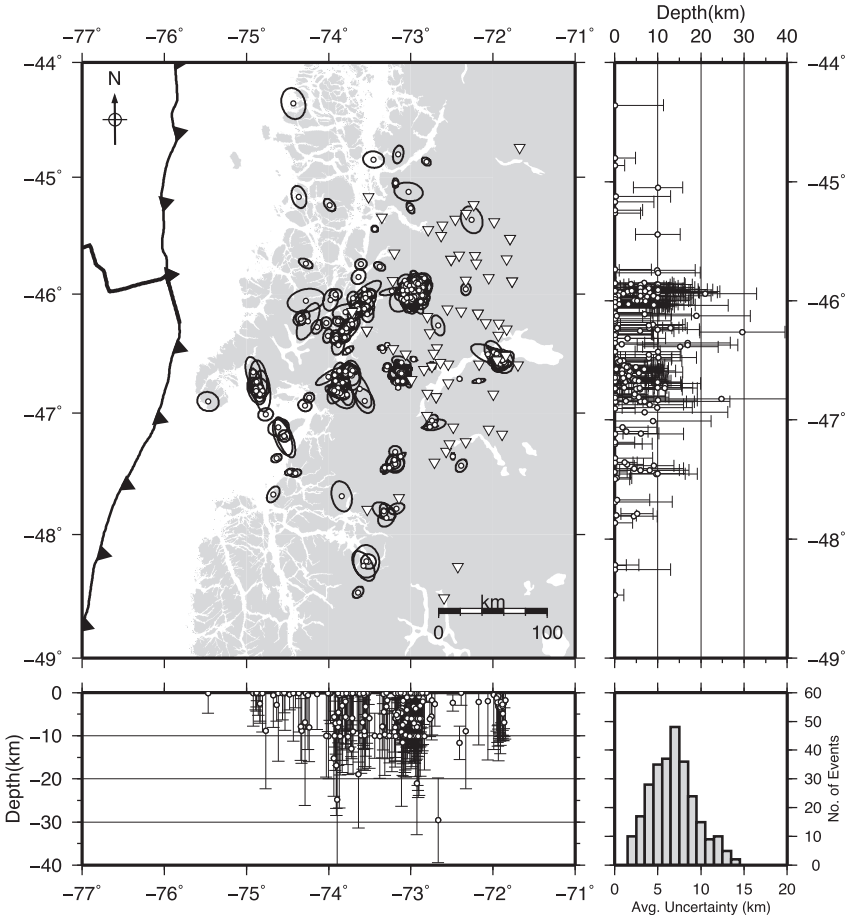


**Fig. 4.** Location uncertainty estimations of events with NonLinLoc uncertainty ellipsoids' semi-axes lesser than 20 km (276 events). Ellipses in plan view and error bars in profiles correspond to 68% confidence location uncertainties. Inverted white triangles indicate seismic stations locations. Histogram shown in lower right corner indicates averaged values from the three semi-axes of the uncertainty ellipsoids.

particular orientation except for those events located near the Taitao Peninsula (~47°S, 75°W), which show ellipses with major axes NW-orientated (see Fig. 4). In particular, Fig. 5 shows clearly the relationship between network disposition and location uncertainty. For example, the smallest uncertainties (red tones) are located where a highest density of stations is deployed, e.g. nearby General Carrera lake. On the other hand, the largest uncertainties (green tones) are located where fewer stations are deployed nearby, e.g. along the coastline and offshore. Although the establishment of this relationship is logical and evident, it is important to highlight that not always all the stations were recording, therefore some events might have been recorded by few stations even though they are located on an area with high density of installed stations.

**Table 1**
1-D velocity model used on the earthquakes location. Taken from Agurto et al. (2012).

| Depth (km)[a] | Vp (km $s^{-1}$) | Vs (km $s^{-1}$) |
|---|---|---|
| 0 | 4.93 | 2.53 |
| 2 | 4.94 | 2.66 |
| 3 | 4.97 | 2.76 |
| 4 | 5.17 | 3.10 |
| 5 | 5.57 | 3.28 |
| 6 | 5.92 | 3.50 |
| 7 | 6.24 | 3.61 |
| 8 | 6.38 | 3.67 |
| 10 | 6.38 | 3.71 |
| 14 | 6.38 | 3.71 |
| 18 | 6.38 | 3.71 |
| 22 | 6.38 | 3.87 |
| 26 | 6.78 | 3.98 |
| 30 | 7.31 | 4.18 |
| 39 | 7.94 | 4.51 |
| 45 | 7.98 | 4.53 |
| 60 | 8.85 | 5.03 |

[a] Top of the layer.

The distribution of seismicity tends to occur in clusters, as shown in Fig. 6 displaying the selected 276 events, which are predominantly distributed in clusters labeled A–F. The rest of the events which are not related to any cluster seem to be mostly associated with shallow crustal activity on the LOFS, and to events sparsely located, at shallow depths and unrelated to any known regional seismic source.

Most of the seismicity nucleates at crustal depths, shallower than 10 km, in particular associated with activity at Hudson volcano (see Cluster A and Discussion sections). Maximum hypocentral depths of 30 km (±8 km) were located, which constrains the seismogenic depth of the region to this value. For the Aysén Fjord area, Agurto et al. (2012) estimated the seismogenic depth to the upper 15 km. This difference might be due to greater uncertainties of the locations in the present research and/or to the nature of the seismicity analyzed in the Aysén Fjord study, exclusively related to the LOFS within a reduced area. In any case, only three events were located beneath 20 km depth in this study, presenting large vertical errors >±9 km (see Fig. 4), with none of them associated with the LOFS. The average uncertainty in the vertical component for the totality of events was ±8.3 km.

Local magnitudes ($M_L$) were obtained in the range of 0.5–3.4. For simplicity, local magnitudes were obtained after the method developed by Richter (1958) using his equation $M_l = \log A - 2{,}48 + 2{,}76 * \log\Delta$ in which A is the maximum displacement (amplitude) in mm, and Δ is the epicentral distance in km for each station. As Richter's equation was derived from Wood–Anderson torsion seismometers response, in this work digital amplitudes were adequately transformed into equivalent Wood–Anderson torsion seismometers displacement by using the software SAC (http://www.iris.edu/software/sac/manual.html) and then introduced into the equation above to calculate the corresponding magnitude.

The largest magnitudes are observed in the vicinity of the CTJ and the southern end of the LOFS, whilst the smallest magnitudes are present in clusters B and D (Fig. 7). Shallow crustal events down to depths of 10 km are located in spatial concordance with the trace of the LOFS, in particular in the area where both the East and West main branches meet at ~46.3°S. This seems to be a highly active seismic zone, with maximum observed magnitudes up to 3.4 $M_l$.

Cluster A is associated with seismic activity at Hudson volcano, representing nearly a third of the total seismicity (85 events out of 276). These events occur mostly within the caldera of the volcano and to the south of it, down to depths of 10 km (Fig. 8). The events that occur within the caldera are located at depths between 6 and

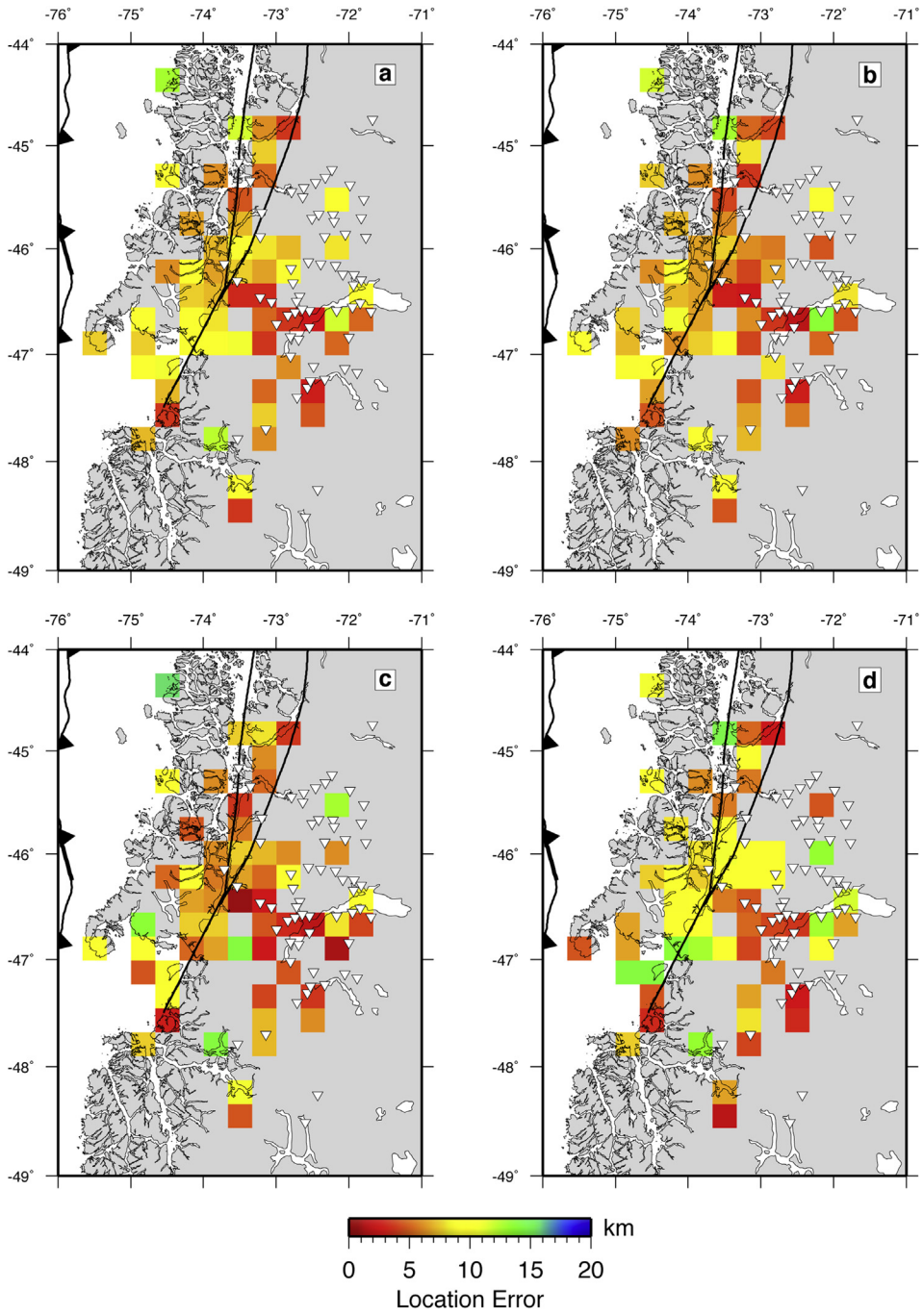


**Fig. 5.** Mean location uncertainties. Averaged uncertainties calculated on a grid of tiles 25 × 25 km for events with error ellipsoids' semi-axes lesser than 20 km (276 events). Error values were calculated from the events' error covariance of latitude, longitude and vertical directions considering a 68% confidence. **a)** averaged latitude, longitude and depth directions error; **b)** longitude error; **c)** latitude error; **d)** vertical error.

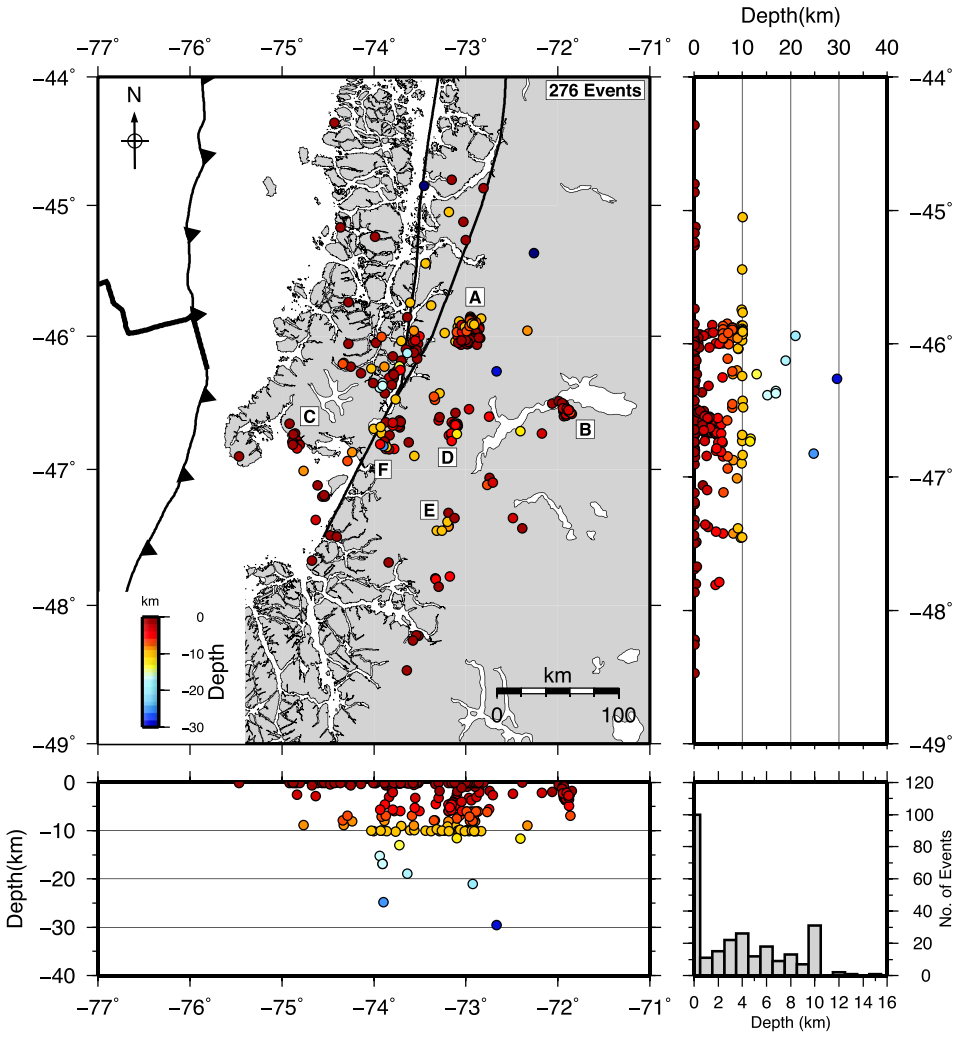


**Fig. 6.** Locations of selected events (error ellipsoids' semi-axes lesser than 20 km) colored by depth. Uppercase letters indicate associated seismic cluster: A Hudson volcano, B Cerro Bayo mine, C CTJ vicinity, D–F glacier events.

10 km, while the events located to the south of the caldera occur at shallower depths. Regarding the temporal distribution of these events, frequencies of 0–10 events per month are observed for the study period, except for February 2004, when up to 33 events related to volcanic activity were recorded (see Fig. 9). Magnitudes fluctuate between 1.4 and 2.9 $M_L$.

Cluster B contains events associated with mining activities in the Cerro Bayo Mine, nearby General Carrera lake. The hypocenters, 31 in total, are located at shallow depths and present magnitudes between 0.6 and 2.3 $M_L$. They also occur at regular times of the day, between 15 and 24 h GMT (11–20 h Local Time). Although these events correspond to mine explosions occurring on the surface, the hypocentral depth range observed is 0–7 km (Fig. 6), providing an independent measure of the vertical uncertainty for our locations (see discussion).

Cluster C corresponds to events located in the vicinity of the CTJ. These events, including the biggest located in the present study, occur at depths shallower than 5 km and show magnitudes of up to 3.4 $M_L$. This seismicity might be associated with activity on the slab-window of the subducted ridge (Murdie et al., 1993), but given its shallow depth, it might also correspond to activity on some shallow crustal structure not recognized previously. The nature and geometry of this structure cannot be constraint from our dataset, thus further research should focus in this area in order to address this point.

Clusters D–F correspond to events that coincide spatially with the presence of glaciers and their terminal zone ending in lakes. Cluster D occurs nearby Fiero Glacier, cluster E in the proximity of Colonia Glacier and cluster F close to Quintín and San Rafael Glaciers; all of them part of the North Patagonian Ice Field. Furthermore, these events present a slight tendency to occur in the summer months (Dec–Feb) as shown in Fig. 10. This suggests the possibility that these epicentres are related to ice calving and avalanches in the mentioned glaciers.

## 4. Discussion

From our study, the regional seismicity in the Aysén Region corresponds mostly to shallow crustal events located in the overriding South American plate at depths shallower than 30 km, mostly within the upper 10 km of crust. No WB zone seismicity associated with the subduction of the Nazca plate was identified during the observational period, contrasting with observations made in the region immediately adjacent to the north of our study area where WB seismicity was found down to at least 70 km depth in a plane dipping 30° to the east (Bohm et al., 2002; Lange et al.,

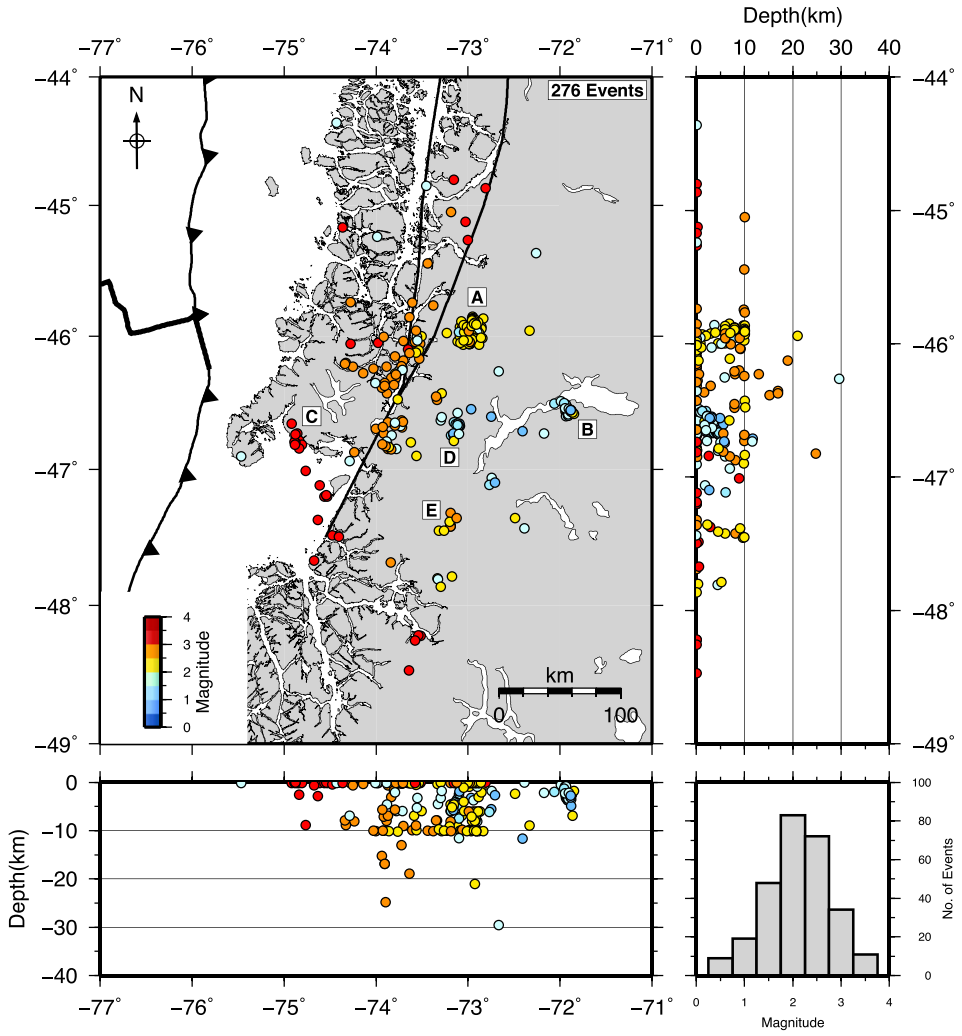


**Fig. 7.** Events shown in Fig. 4 colored by local magnitude. Uppercase letters indicate associated cluster (see text and Fig. 6).

2007). The lack of deep earthquakes and a clear WB zone in our area can be related to the subduction of a very young and hot oceanic crust as suggested previously (e.g. Kirby et al., 1996).

The seismicity in the region is mainly related to activity at Hudson volcano, which represents a third of the levels of seismicity in the area. These events occur within the caldera of the volcano and in a cluster ~5 km to the south of it, at depths between 0 and 10 km. In this regard, these results partially disagree with Naranjo et al. (1993), who reported hypocentral depths clustered between 2 and 20 km, although both works are not directly comparable since Naranjo et al.'s study was performed during the Hudson eruptive sequence of 1991 and using a different seismic network configuration. Unfortunately, it is not possible to clearly state whether the Hudson events found in the present study are of tectonic or volcanic origin. It is worth noticing though that waveforms from these events do not present any signal associated with magma/fluid migration (long period events) or volcanic tremors, and that during the research period no volcanic activity was reported to our knowledge. Likely these events are related to rock fracturing, being part of the normal seismic activity that this volcano presents as periodically reported by the Chilean volcanic monitoring network (http://www.sernageomin.cl/volcanes.php).

The second source of background seismicity in the region is related to the LOFS, which represents an active fault system during the time of this study (2004–2005) with magnitudes of up to 3.4 $M_L$, but as reported previously (e.g. Sepúlveda and Serey, 2009; Mora et al., 2010; Legrand et al., 2011; Russo et al., 2011; Agurto et al., 2012) it is capable of generate earthquakes of at least $M_W$ 6.2, representing a significant seismic hazard in the region. The activity on the LOFS is particularly intense in the area of convergence of the two main branches of the fault at ~46.3°S. During the period of this experiment (2004–2005), no seismicity was observed in the area of the Aysén Fjord where the sequence of 2007 took place.

Focal mechanisms would be necessary to associate with more certainty some of the events either to the LOFS or other seismotectonic sources in the area, as well as to address the distribution of stresses and faulting geometries in the region. Given the low magnitudes and low S/N ratio of the processed events, moment tensor inversions were not reliably obtained, neither focal mechanisms from first motion polarities given that most of the events spatially associated with the LOFS fell outside the seismic network, and when the azimuthal coverage was smaller than 180° for some events, the shallow occurrence of these events only contributed to a very narrow range of observed incidence angles.

Seismic activity was also recorded in the Taitao Peninsula and nearby area (cluster C). This zone was previously studied by Murdie et al. (1993), who inferred that this seismicity was caused by the

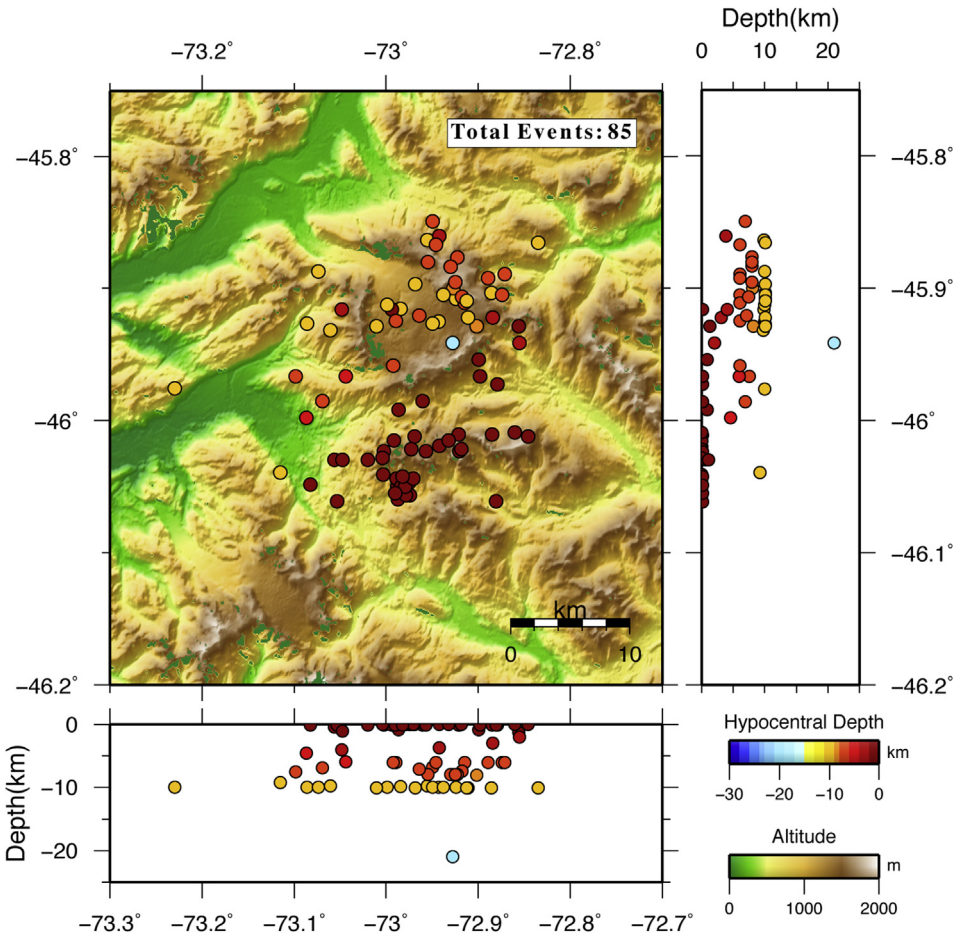


**Fig. 8.** Hudson volcano related events colored by depth.

subduction of the active ridge bellow South America. In particular, they managed to constrain focal mechanisms obtaining for all of them extensional faulting associated with the subducted spreading center. Thus, the seismicity observed in that area (cluster C) in the present study might also correspond to activity on the subducted ridge that seems to continue active after subduction in the CTJ.

Minor seismicity was also observed spatially related to several glaciers within the North Patagonian Ice Field. These events would be associated with ice calving on the terminal zones of the glaciers and/or avalanches in the areas of steep slopes. Given the small magnitudes, these events were only detectable because of the presence of nearby seismic stations.

Lastly, a few events were located offshore, associated with the ridge system (see Sup. Fig. 1). Due to its large uncertainties (events located far and outside the network), these events were not included in our final catalog of 276 events.

Unfortunately, given that the design of the seismic network was conceived for a receiver functions experiment, the coverage was not ideal to constrain with more accuracy the local seismicity. This is reflected on the vertical uncertainties that can be independently inferred to be ±7 km in the area around Cerro Bayo mine. Another important problem contributing to high uncertainties was the difficult installation and operation of stations, in particular during the winter months, due to accessibility and weather issues.

Future seismic research in the area should be aimed at obtaining focal mechanisms and the collection of offshore data, and therefore, an improved station coverage, in order to better constrain the seismotectonic processes in the area and dominant stress field. Furthermore, additional geological mapping of structures and re-estimation of geological hazards are necessary in order to obtain a complete picture of the seismotectonics of this region both at a local level and as a unique example of an area in which young crust and an active triple junction is subducted under continental crust bisected by a major strike-slip fault such as the LOFS.

## 5. Conclusions

We have recorded and characterized the local seismicity for the area in the vicinity of the Chile Triple Junction between 44°S and 49°S during the years 2004–2005. Our data come to fill a gap existent until now in terms of local seismicity studies for this region. A total of 519 events were detected, with a high quality subset of 276 events with error ellipsoid semi-axes lesser than 20 km. Magnitudes vary in the range of 0.5–3.4 $M_L$.

Only intra-plate crustal events were detected with shallow depths mostly down to 10 km. Earthquake clustering seems to be the characteristic type of occurrence in this region, whilst no Wadati–Benioff seismicity was observed during the observation period.

The main source of seismic activity in the region corresponds to the Hudson volcano with approximately one third of the total seismicity and depths of 0–10 km. Sparse events are associated with activity on the LOFS, in particular a high concentration is observed where the two main branches meet, at ~46.2°S. Other clustered shallow events with low magnitude were spatially associated with the terminal parts of glaciers, probably related to glacier

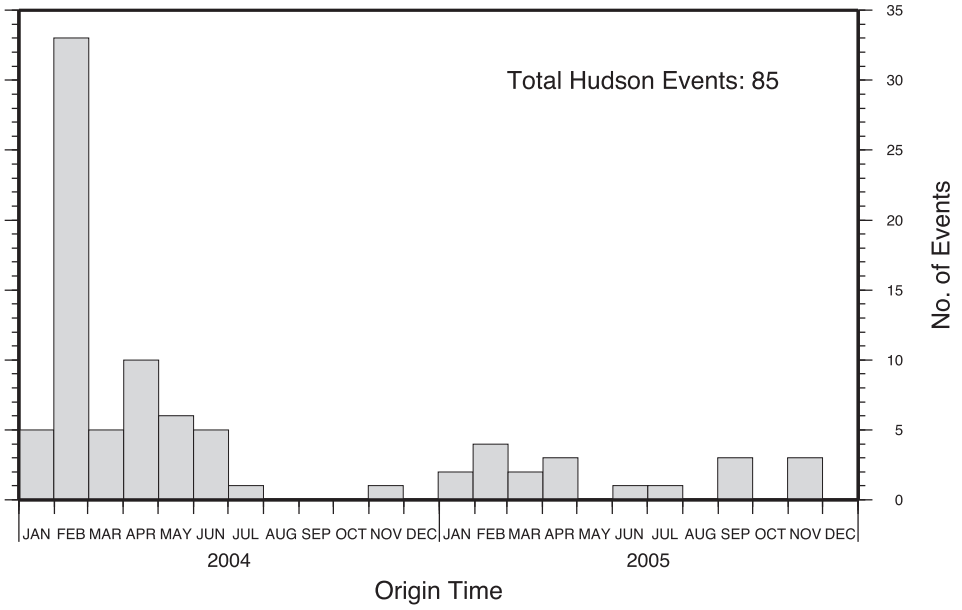


**Fig. 9.** Histogram of time occurrence of events associated with the Hudson volcano distributed in monthly bins.

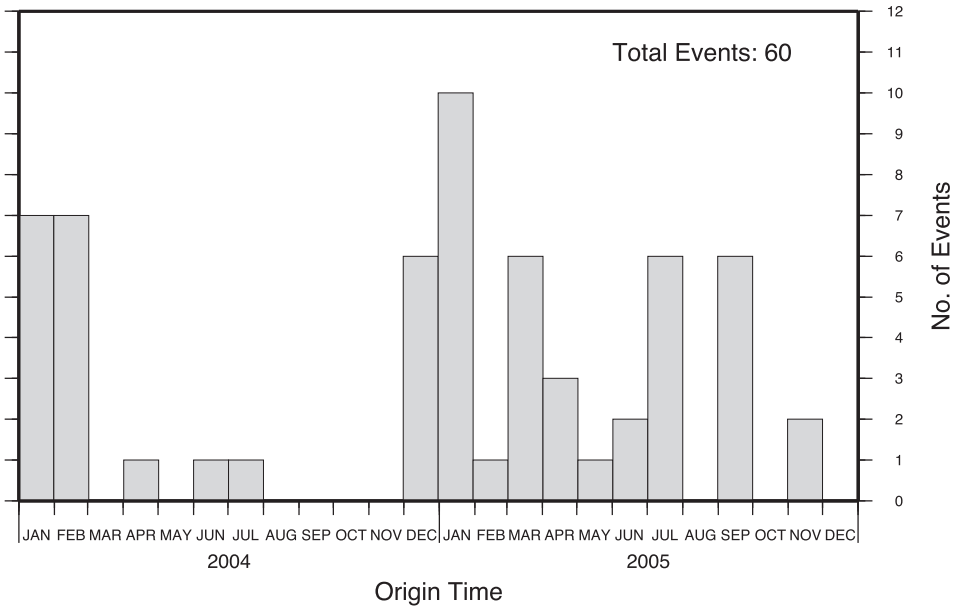


**Fig. 10.** Histogram of time occurrence of glacier related events distributed in monthly bins.

calving during the summer months. Few events occur in the area nearby the subduction of the CTJ, although the location uncertainties in this area are too large for a more detailed investigation.

In conclusion, the 'normal' background seismicity of this region presents crustal events shallower than 15 km and maximum magnitudes up to 4. Episodically, during eruptive phases of the Hudson volcano or reactivation of the LOFS as in 2007, maximum magnitudes can reach M ~ 7, representing a significant hazard in this region, which should be taken into account in future assessments.

## Acknowledgments

We wish to thank the Chilean Police, Army, Navy and National Emergency Office (ONEMI) for their assistance with the deployment and servicing of the SEARCH seismic network, as well as many students from the University of Concepcion without whom this work would have not been possible. SEIS-UK are thanked for providing the seismic equipment used in this study and the data management procedures used to create the initial dataset. We also thank José Cembrano and an anonymous reviewer for his/her valuable comments. This work was partially supported by Conicyt, Chile for H.A. and by JSPS KAKENHI Grant Number 13373004 for H.I. Some of the figures were made with the software GMT (Wessel and Smith, 1998).

## Appendix A. Supplementary material

Supplementary data related to this article can be found online at http://dx.doi.org/10.1016/j.jsames.2013.12.011.

## References


Agurto, H., Rietbrock, A., Barrientos, S., Bataille, K., Legrand, D., 2012. Seismotectonic structure of the Aysén Region, Southern Chile, inferred from the 2007 $M_w = 6.2$ Aysén earthquake sequence. Geophys. J. Int. 190, 116–130. http://dx.doi.org/10.1111/j.1365-246X.2012.05507.x.

Behrmann, J., Lewis, S., Cande, S., 1994. Tectonics and geology of spreading ridge subduction at the Chile triple junction: a synthesis of results from leg 141 of the ocean drilling program. Geol. Rundsch. 83 (4), 832–852.

Bohm, M., Lüth, S., Echtler, H., Asch, G., Bataille, K., Bruhn, C., Rietbrock, A., Wigger, P., 2002. The Southern Andes between 36° and 40°S latitude: seismicity and average seismic velocities. Tectonophysics 356 (4), 275–289.

Cande, S., Leslie, R., 1986. Late Cenozoic tectonics of the southern Chile trench. J. Geophys. Res. 91, 471–496.

Cande, S., Leslie, R., Parra, J., Hobart, M., 1987. Interaction between the Chile Ridge and Chile Trench: geophysical and geothermal evidence. J. Geophys. Res. 92, 495–520.

Cembrano, J., Moreno, H., 1994. Geometría y naturaleza contrastante del volcanismo cuaternario entre los 38°S y 46°S: dominios compresionales y tensionales en un régimen transcurrente. In: Congreso Geologico Chileno, vol. 7, pp. 17–21. Concepción.

Cembrano, J., Hervé, F., Lavenu, A., 1996. The Liquine–Ofqui fault zone: a long-lived intra-arc fault system in southern Chile. Tectonophysics 259, 55–66.

Cembrano, J., Schermer, E., Lavenu, A., Sanhueza, A., 2000. Contrasting nature of deformation along an intra-arc shear zone, the Liquiñe-Ofqui Fault System, Southern Chilean Andes. Tectonophysics 319, 129–149.

Cembrano, J., Lavenu, A., Reynolds, P., Arancibia, G., López, G., Sanhueza, A., 2002. Late Cenozoic transpressional ductile deformation north of the Nazca-South America-Antarctica triple junction. Tectonophysics 354, 289–314.

Cembrano, J., Lara, L., 2009. The link between volcanism and tectonics in the southern volcanic zone of the Chilean Andes: a review. Tectonophysics 471 (1–2), 96–113. http://dx.doi.org/10.1016/j.tecto.2009.02.038.

Comte, D., Gallego, A., Russo, R., Murdie, R., VanDecar, J., 2007. The Aysen (Southern Chile) 2007 seismic swarm: volcanic or tectonic origin? EOS Trans. Am. Geophys. Un. 88 (23). Jt Assem. Suppl., Abstract S43C-04.

D'Orazio, M., Innocenti, F., Manetti, P., Tamponi, M., Tonarini, S., Gonzalez-Ferran, O., Lahsen, A., Omarini, R., 2003. The quaternary calc-alkaline volcanism of the Patagonian Andes close to the Chile triple junction: geochemistry and petrogenesis of volcanic rocks from the Cay and Maca volcanoes (~45°S, Chile). J. S. Am. Earth Sci. 16 (4), 219–242. http://dx.doi.org/10.1016/S0895-9811(03)00063-4.

Forsythe, R., Nelson, E., 1985. Geological manifestations of ridge collision: evidence from the Golfo de Penas-Taitao basin, southern Chile. Tectonics 4 (5), 477–495.

Forsythe, R., Nelson, E., Carr, M., Keading, M., Hervé, M., Mpodozis, C., Soffia, J., Harambour, S., 1986. Pliocene near trench magmatism in Southern Chile: a possible manifestation of ridge collision. Geology 14, 23–27.

Gallego, A., Russo, R.M., Comte, D., Mocanu, V.I., Murdie, R.E., Vandecar, J.C., 2010. Seismic noise tomography in the Chile ridge subduction region. Geophys. J. Int. 182 (3), 1478–1492. http://dx.doi.org/10.1111/j.1365-246X.2010.04691.x.

Gorring, M., Kay, S., Zeitler, P., Ramos, V., Rubiolo, D., Fernandez, M., Panza, J., 1997. Neogene Patagonian plateau lavas: continental magmas associated with ridge collision at the Chile Triple Junction. Tectonics 16 (1), 1–17.

Greve, F., 1964. Historia de la Sismología en Chile. Instituto de Geofísica y Sismología, Universidad de Chile, p. 138 (unpublished).

Herron, E., Cande, S., Hall, B., 1981. An active spreading center collides with a subduction zone: a geophysical survey of the Chile Margin Triple Junction. In: Nazca Plate: Crustal Formation and Andean Convergence. Geol. Soc. Am. Mem, vol. 154, pp. 683–702.

Kirby, S., Engdahl, E.R., Denlinger, R., 1996. Intermediate-depth intraslab earthquakes and arc volcanism as physical expressions of crustal and uppermost mantle metamorphism in subducting slabs. In: Bebout, G.E., Scholl, D.W., Kirby, S.H., Platt, J.P. (Eds.), Subduction Top to Bottom, Geophysical Monograph Series. American. Geophysical Union, Washington D.C, pp. 195–214.

Lange, D., Rietbrock, A., Haberland, C., Bataille, K., Dahm, T., Tilmann, F., Flüh, E., 2007. Seismicity and geometry of the south Chilean subduction zone (41.5°S–43.5°S): Implications for controlling parameters. Geophys. Res. Lett. 34, L06311. http://dx.doi.org/10.1029/2006GL029190.

Lange, D., Cembrano, J., Rietbrock, A., Haberland, C., Dahm, T., Bataille, K., 2008. First seismic record for intra-arc strike-slip tectonics along the Liquiñe-Ofqui fault zone at the obliquely convergent plate margin of the Southern Andes. Tectonophysics 455, 14–24. http://dx.doi.org/10.1016/j.tecto.2008.04.014.

Legrand, D., Barrientos, S., Bataille, K., Cembrano, J., Pavez, A., 2011. The fluid-driven tectonic swarm of Aysen Fjord, Chile (2007) associated with two earthquakes ($M_w = 6.1$ and $M_w = 6.2$) within the Liquiñe Ofqui Fault Zone. Cont. Shelf Res. 31, 154–161. http://dx.doi.org/10.1016/j.csr.2010.05.008.

Lomax, A., Virieux, J., Volant, P., Berge, C., 2000. Probabilistic Earthquake Location in 3D and Layered Models: Introduction of a Metropolis–Gibbs Method and Comparison with Linear Locations in Advances in Seismic Event Location. Springer, Amsterdam, pp. 101–134.

Melnick, D., Bookhagen, B., Strecker, M.R., Echtler, H., 2009. Segmentation of megathrust rupture zones from forearc deformation patterns over hundreds to millions of years, Arauco Peninsula. J. Geophys. Res. 114, B01407. http://dx.doi.org/10.1029/2008JB005788.

Miller, M., Bataille, K., Priestley, K., Iwamori, H., Calisto, I., 2005. Seismic imaging of a subducted ridge, southern Chile. EOS Trans. Am. Geophys. Un. 86, 52. Fall Meet. Suppl., Abstract S51A-0982.

Mora, C., Comte, D., Russo, R., Gallego, A., Mocanu, V., 2010. Aysén seismic swarm (January 2007) in southern Chile: analysis using joint hypocentral determination. J. Seismol. 14 (4), 683–691. http://dx.doi.org/10.1007/s10950-010-9190-y.

Murdie, R., Prior, D., Styles, P., Flint, S., Pearce, R., Agar, S., 1993. Seismic responses to ridge-transform subduction: Chile triple junction. Geology 21 (12), 1095–1098.

Naranjo, J.A., Moreno, H., Banks, N., 1993. La erupción del volcán Hudson en 1991 (46°S), Región XI, Aisén, vol. 44. Servicio Nacional de Geología y Minería, Santiago.

Naranjo, J.A., Stern, C., 1998. Holocene explosive activity of Hudson volcano, southern Andes. Bull. Volcanol. 59 (4), 291–306.

Niemeyer, H., Skármeta, J., Fuenzalida, R., Espinosa, W., 1984. Hojas Península de Taitao y Puerto Aisén, Carta Geológica de Chile, 60–61, 1 mapa escala 1: 500.000. Servicio Nacional de Geología y Minería, Santiago.

Pankhurst, R.J., Weaver, S.D., Hervé, F., Larrondo, P., 1999. Mesozoic-cenozoic evolution of the North Patagonian batholith in Aysén, Southem Chile. J. Geol. Soc. Lond. 156, 673–694.

Plafker, G., Savage, J.C., 1970. Mechanism of the Chilean earthquake of May 21 and 22, 1960. Geol. Soc. Am. Bull. 81, 1001–1030.

Ramos, V., Kay, S., 1992. Southern Patagonian Plateau basalts and deformation: back-arc testimony of ridge collision. Tectonophysics 205, 261–282.

Richter, C.F., 1958. Elementary Seismology. Freeman and Co., San Francisco.

Rosenau, M., Melnick, D., Echtler, H., 2006. Kinematic constraints on intra-arc shear and strain partitioning in the Southern Andes between 38°S and 42°S latitude. Tectonics 25 (4), TC4013. http://dx.doi.org/10.1029/2005TC001943.

Russo, R.M., Gallego, A., Comte, D., Mocanu, V.I., Murdie, R.E., Vandecar, J.C., 2010a. Source-side shear wave splitting and upper mantle flow in the Chile ridge subduction region. Geology 38 (8), 707–710. http://dx.doi.org/10.1130/G30920.1.

Russo, R., Vandecar, J.C., Comte, D., Mocanu, V.I., Gallego, A., Murdie, R.E., 2010b. Subduction of the Chile ridge: upper mantle structure and flow. GSA Today, 4–10. http://dx.doi.org/10.1130/GSATG61A.1.

Russo, R.M., Gallego, A., Comte, D., Mocanu, V.I., Murdie, R.E., Mora, C., VanDecar, J.C., 2011. Triggered seismic activity in the Liquiñe-Ofqui fault zone, Southern Chile, during the 2007 Aysen seismic swarm. Geophys. J. Int. 184, 1317–1326. http://dx.doi.org/10.1111/j.1365-246X.2010.04908.x.

Sepúlveda, S., Serey, A., 2009. Tsunamigenic, earthquake-triggered rock slope failures during the 21st of April 2007 Aysén earthquake, southern Chile (45.5°S). Andean Geol. 36 (1), 131–136.

SERNAGEOMIN, 2003. Mapa Geológico de Chile: versión digital, 4 (CD-ROM, versión1.0, 2003), 1 mapa geológico de Chile escala 1:1.000.000. Servicio Nacional de Geología y Minería, Santiago.

Thomson, S.N., 2002. Late Cenozoic geomorphic and tectonic evolution of the Patagonian Andes between latitudes 42°S and 46°S: an appraisal based on fission-track results from the transpressional intra-arc Liquiñe-Ofqui fault zone. Geological Soc. Am. Bull. 114 (9), 1159–1173.

Wang, K., Hu, Y., Bevis, M., Kendrick, E., Smalley Jr., R., Vargas, R., Lauría, E., 2007. Crustal motion in the zone of the 1960 Chile earthquake: detangling earthquake-cycle deformation and forearc-sliver translation. Geochem. Geophys. Geosyst. 8, Q10010. http://dx.doi.org/10.1029/2007GC001721.

Wessel, P., Smith, W., 1998. New, improved version of generic mapping tools released. EOS Trans. Am. Geophys. Un. 79, 579. http://dx.doi.org/10.1029/98EO00426, 579.

Wortel, M.J.R., Vlaar, N.J., 1978. Age-dependent subduction of oceanic lithosphere beneath western South America. Phys. Earth Planet. Inter 17, 201–208.